2008

NiCo2O4/C Nanocomposite as a highly reversible anode material for lithium-ion batteries

Yanna NuLi
University of Wollongong, yanna@uow.edu.au

Peng Zhang
University of Wollongong

Zaiping Guo
University of Wollongong, zguo@uow.edu.au

Hua-Kun Liu
University of Wollongong, hua@uow.edu.au

Jun Yang
Shanghai Jiao Tong University

Electrochemical and Solid-State Letters, **11** (5) A64-A67 (2008)
1099-0062/2008/11(5)/A64/4/$23.00 © The Electrochemical Society

$NiCo_2O_4$/C Nanocomposite as a Highly Reversible Anode Material for Lithium-Ion Batteries

Yanna NuLi,[a,b,z] Peng Zhang,[b] Zaiping Guo,[b,z] Huakun Liu,[b,*] and Jun Yang[a,*]

[a]*Department of Chemical Engineering, Shanghai Jiao Tong University, Shanghai 200240, China*
[b]*Institute for Superconducting and Electronic Materials, University of Wollongong, Wollongong, New South Wales 2522, Australia*

A $NiCo_2O_4$/C nanocomposite has been synthesized by a hydrothermal method followed by a calcination. X-ray powder diffraction and transmission electron microscopy measurements demonstrated the composite was composed of crystalline $NiCo_2O_4$ and amorphous carbon, and $NiCo_2O_4$ and carbon particles amalgamated together with good affinity. The electrochemical results showed as high as 914.5 mAh/g reversible capacity could be achieved at 40 mA/g current density in the potential range of 0.01−3.0 V. The initial coulombic efficiency of the composite was 79.2%, and the capacity retention was 78.3% up to 50 cycles. The superior electrochemical performance indicated that the $NiCo_2O_4$/C nanocomposite might be a promising alternative to conventional graphite-based anode materials for lithium-ion batteries.
 [DOI: 10.1149/1.2861226]

Manuscript submitted November 14, 2007; revised manuscript received January 9, 2008. Available electronically March 3, 2008.

During the past decade, research on anode materials for lithium-ion batteries mainly focused on searching for carbon alternatives with larger capacities and better cycling performances.[1,2] Conversion reactions have opened a new line of research in the field of electrode materials for Li-ion batteries. It was found that transition-metal oxides (MO, where M is Co, Ni, Cu, or Fe) can be reduced to their metal state and then be reoxidized, providing a large reversible capacity (700 mAh/g), good cycling performance, and high recharge rates.[3] The reaction mechanism of these metal oxides by lithium involved the reversible reduction and oxidation of metal (M) nano-sized particles dispersed into a lithia matrix (Li_2O), followed by the formation/decomposition of a solid electrolyte interface (SEI). It was found that the electrochemical properties of the electrodes were related to factors such as the large change in volume, the serious aggregation or pulverization of active particles during charge–discharge, and poor conductivity of the transition metal oxides.[4] In previous work, it has further been proposed that mixed transition metal oxides such as $NiCo_2O_4$,[5] $NiFe_2O_4$,[6] and $CoFe_2O_4$,[7-9] can react reversibly with larger amounts of lithium and the preparation methods have a crucial effect on electrochemical performance in long-term cycling.[7]

Due to its relatively high electrical conductivity and infrared transparency, $NiCo_2O_4$ has been developed as an alternative electrode material for supercapacitors[10-12] and used as a heterogeneous optical recording media.[13] Moreover, the electrochemical properties have been studied widely in alkaline medium for the oxygen evolution reaction. The preparation methods include thermal decomposition,[5,14] solution deposition,[15] combinatorial sputtering deposition,[16] single-target sputter deposition,[16] and hydroxide coprecipitation,[17] etc.

It is well known that hydrothermal synthesis has been shown to be advantageous over other methods in homogeneous nucleation and grain growth.[18] In the work reported here, we describe an easy route to isochronously synthesize $NiCo_2O_4$/C nanocomposite via a low-temperature hydrothermal method followed by calcination, using poly(ethylene glycol) as the carbon source. $NiCo_2O_4$ was combined with nearly 8Li and exhibited a high discharge capacity,[5] and carbon was introduced to suppress the aggregation of the metal oxide and increase conductivity. The composite displays outstanding electrochemical activity, with 79.2% initial coulombic efficiency, 914.5 mAh/g reversible capacity, and 78.3% capacity retention upon 50 cycles at 40 mA/g. As far as we know, it is the first report about the composite as an anode material for lithium-ion batteries.

Experimental

Preparation of $NiCo_2O_4$/C composite.— All the chemical reagents were analytically pure and used without further purification. In a typical experimental procedure, polyethylene glycol (PEG-600, Aldrich) was dissolved in methanol to 2 M solution. $Ni(NO_3)_2 \cdot 6H_2O$ (1 M) and $Co(NO_3)_2 \cdot 6H_2O$ (1 M) aqueous solution with a 1:2 Co/Ni molar ratio was added dropwise into equivalent molar number PEG-600 solution under continuous stirring at room temperature to obtain a homogeneous precursor solution. A stoichiometric proportion of the precursor and NaOH (4 M) was added under stirring to a 15 mL Teflon-lined autoclave and filled one-half by volume. The autoclave was sealed and heated at 160°C for 24 h and then cooled naturally. The resulting product was separated by centrifugation, washed with ethanol and distilled water to ensure total removal of the inorganic ions, and then dried under vacuum at 80°C for 4 h as the intermediate product. After that, the intermediate product was calcinated at 300°C for 2 h in argon.

Sample characterizations.— X-ray powder diffraction analysis was conducted on a Philips 1730 X-ray diffractometer (XRD) using Cu Kα radiation (λ = 1.54056 Å) with 2θ ranging from 10 to 80° to analyze the structure of the expected product. A JEOL 2011 200 KeV transmission electron microscope (TEM) with energy-dispersive spectroscopy (EDS) and EDS X-ray mapping was employed to examine the morphology and analyze the product elements.

Electrodes were prepared by drying the slurry of 70 wt % active material, 15 wt % carbon black, and 15 wt % polyvinylidene fluoride dissolved in *N*-methyl-2-pyrrolidinone on a copper foil (1 cm^2) at 100°C for 4 h under vacuum. Electrochemical behavior of the test materials was examined via CR2025 coin cells with lithium metal counter electrode, Celgard 2700 membrane separator, and 1 M $LiPF_6$ electrolyte dissolved in a mixture of ethylene carbonate and dimethyl carbonate with a 1:1 weight ratio. The cells were assembled in an argon-filled glove box (Mbraun, Unilab, Germany). The galvanostatic charge–discharge measurements were conducted at ambient temperature on a multichannel battery cycler with a cut-off voltage of 0.01/3.0 V vs Li/Li^+ under a current density of 40 mA/g. Cyclic voltammetry (CV) measurements of the electrode were performed on a CHI Electrochemical Workstation (CHI Instruments) with a scan rate of 1 mV/s between 0.01 and 3.0 V vs Li/Li^+.

Results and Discussion

The XRD pattern of the as-synthesized powder is shown in Fig. 1. The diffraction peaks at 31.27, 36.26, 44.19, 59.35, 65.23, and 76.70° can be indexed as the (220), (311), (400), (511), (440), and (622) crystal planes of the spinel structure of $NiCo_2O_4$ (JCPDS No. 73–1702), respectively. There was no diffraction peak corresponding

* Electrochemical Society Active Member.
[z] E-mail: nlyn@sjtu.edu.cn; zguo@uow.edu.au

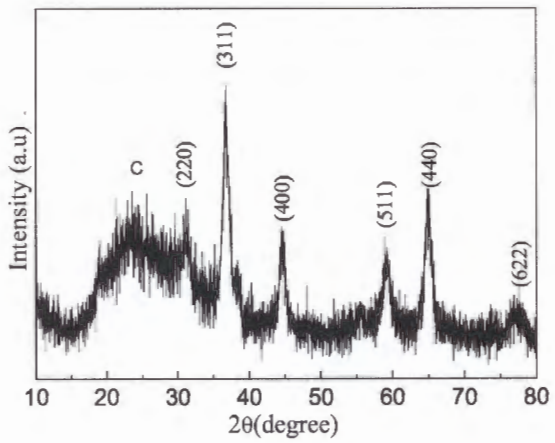

Figure 1. XRD pattern of as-prepared $NiCo_2O_4$/C nanocomposite.

to another Ni- or Co-containing compound, indicating the formation of a single-phase $NiCo_2O_4$. The broad diffraction peak at about 24° corresponds to the amorphous carbon. The result indicates the product is a composite composed of $NiCo_2O_4$ and carbon.

Figure 2 shows the TEM images of the as-synthesized $NiCo_2O_4$/C composite with different magnification. It can be clearly seen that fine particles with particle size of 10–20 nm are distributed in a brighter matrix (Fig. 2a). Based on EDS analysis, it is found that the fine particles which appear dark are $NiCo_2O_4$, while the brighter matrix is carbon. Figures 2b and c present higher magnification images. It can be observed that the $NiCo_2O_4$ particles are mainly located in the inner region, while a small amount of $NiCo_2O_4$ particles are embedded in the brighter matrix. The results suggest that the $NiCo_2O_4$ particles are surrounded by a thin layer of amorphous carbon or are embedded in the amorphous carbon. It is reasonable to believe that $NiCo_2O_4$ particles have completely amalgamated with carbon particles and there is good interface affinity between them. Selected area electron diffraction (SAED) in the inset of Fig. 2c consisted of spots and diffused hales, suggesting that crystalline $NiCo_2O_4$ particles coexist within the amorphous carbon matrix, which is consistent with the XRD result.

The detailed elemental distribution was evaluated to investigate the elemental distribution in the composite. Figure 3a is a TEM image, Fig. 3b-e shows the corresponding EDS mapping for Ni, Co, O, and C elements, respectively. The bright spots correspond to the presence of each element. It is obvious that the distribution of carbon in the composite is homogeneous. The representative EDS analysis (Fig. 3f) reveals that the content of Ni and Co is 12.60 and 25.85 mol %, respectively, close to the stoichimetric molar ratio of 1:2 in the spinel. The carbon content in the composite is as high as 14.68 mol %.

Figure 4 shows the CV curves of the $NiCo_2O_4$/C nanocomposite electrode cycled between 0.01 and 3.0 V at a sweep rate of 1 mV/s. During the first cycle, a reduction peak appears at about 0.62 V, which can be attributed to the decomposition of $NiCo_2O_4$ into Ni and Co, and the formation of amorphous Li_2O and the SEI.[5] Moreover, the two oxidation peaks located at about 1.74 and 2.33 V can be attributed to the reverse process where metals are reoxidized to oxides and Li_2O decomposes.[5] In the subsequent cycle, the oxidation peaks keep the potential, although the reduction peak becomes broad and shifts up to around 0.83 V. The peak intensity remains almost steady after decreasing during the first several cycles.

Figure 5 shows the charge/discharge curves of $NiCo_2O_4$/C nanocomposite electrode cycled between 0.01 and 3.0 vs Li/Li^+ at 40 mA/g. In the first discharge process, the potential rapidly falls and reaches a long voltage plateau at around 1.02 V, followed by a gradual decrease to 0.01 V, and 1154.2 mAh/g initial discharge capacity can be obtained. The first charge process exhibits a higher and

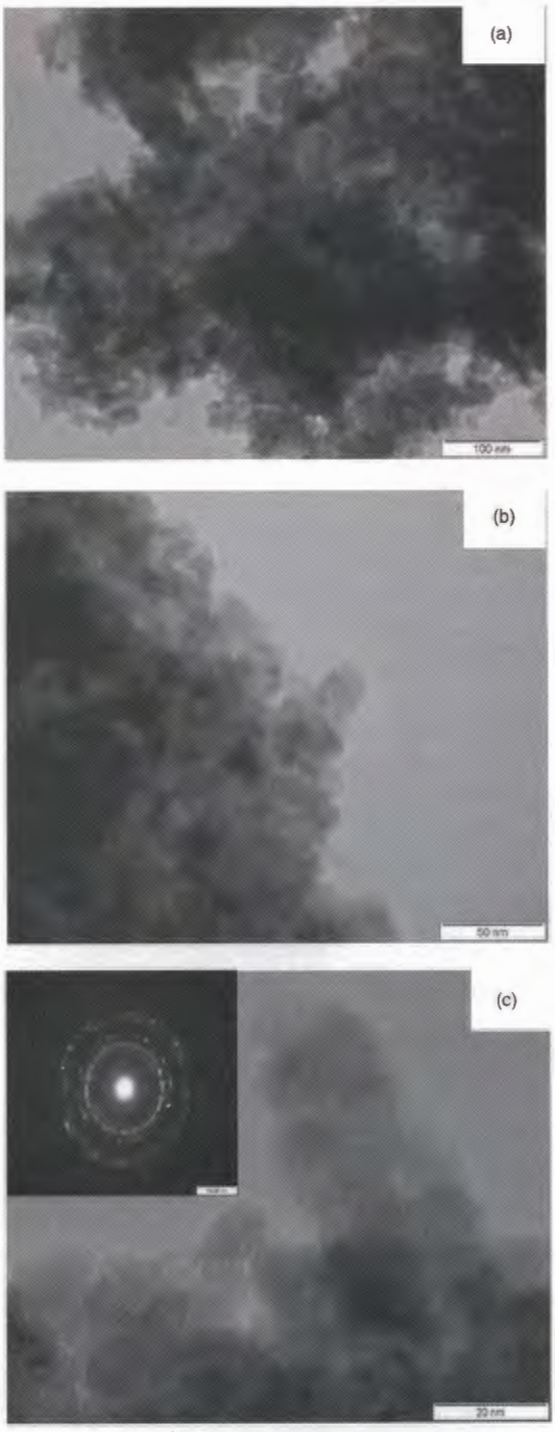

Figure 2. TEM images of an as-prepared $NiCo_2O_4$/C nanocomposite with different magnification. The inset is the corresponding SAED pattern.

sloping voltage profile, with two unconspicuous plateaus and less capacity of 914.5 mAh/g with 79.2% initial coulombic efficiency. The irreversible capacity occurring during the first cycle can be attributed to the decomposition of both the SEI and Li_2O. In the subsequent cycles, the large irreversible capacity is not observed. The voltage plateau appears at a higher voltage of about 1.1 V, the amplitude of the plateau reduces in the discharge process, and a high reversible capacity of 958.4 mAh/g can be achieved.

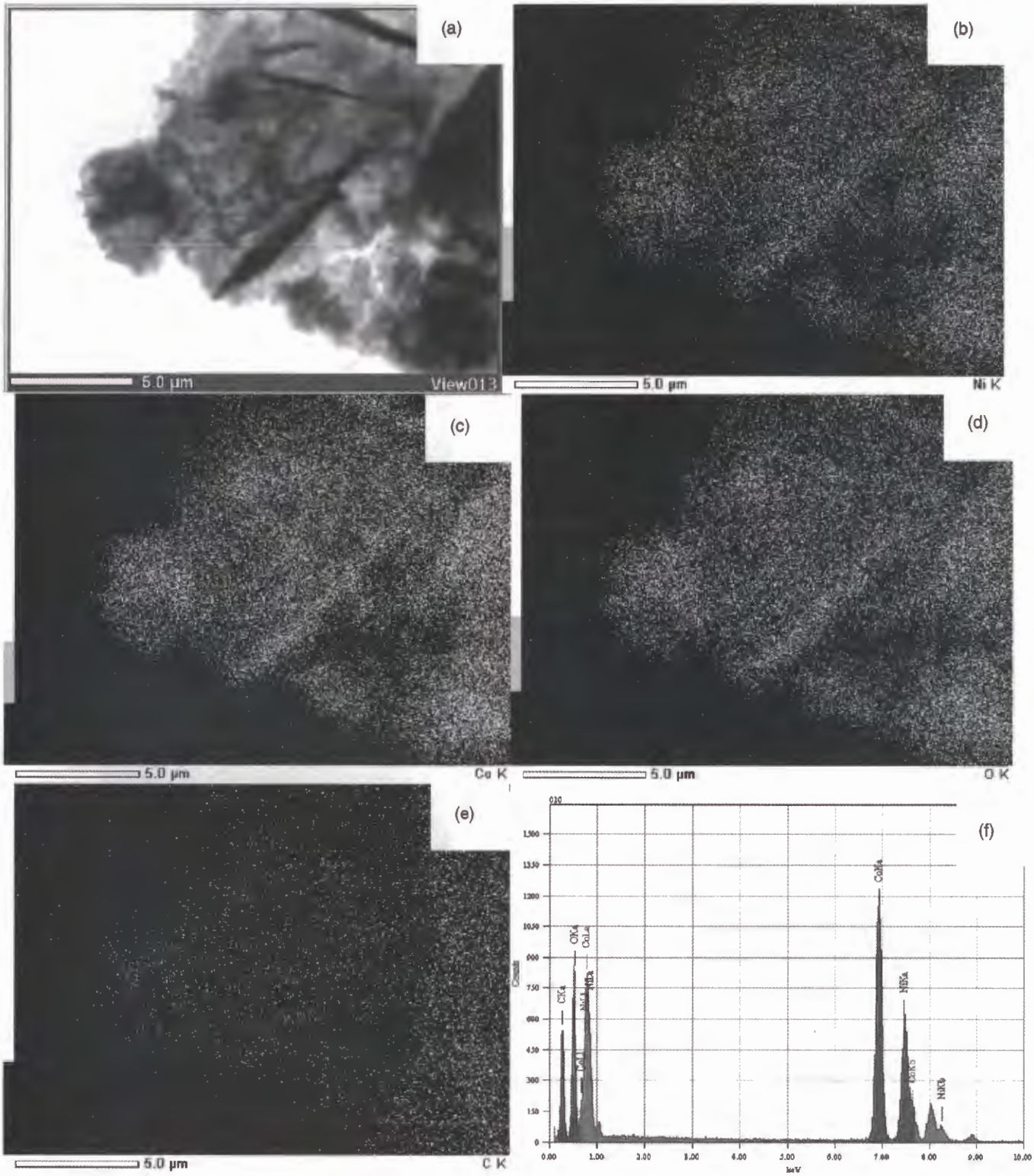

Figure 3. (Color online) A TEM image (a) and corresponding EDS mapping for Ni (b), Co (c), O (d), and C (e) elements and the corresponding EDS spectrum (f).

Figure 6 presents the cycling behavior of the $NiCo_2O_4$/C nanocomposite electrode. The capacity can be maintained at 715.8 mAh/g after 50 cycles, which is about 78.3% of the reversible capacity. There is no serious capacity fading, suggesting that no observable structural degradation takes place during repeated cycling. Compared with those of $NiCo_2O_4$ electrodes reported in literature,[5] the capacity retention and the initial coulombic efficiency of the $NiCo_2O_4$/C nanocomposite prepared in this work are better. The excellent electrochemical performance of the composite could be attributed to the complete amalgamation of $NiCo_2O_4$ particles and

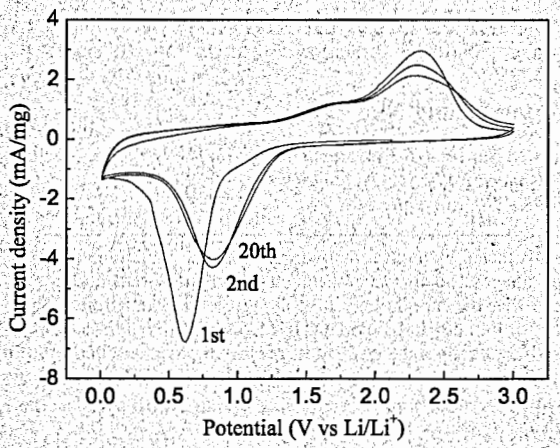

Figure 4. CV results of the $NiCo_2O_4$/C nanocomposite electrode at a scan rate of 1 mV/s.

carbon particles. The good interface affinity between $NiCo_2O_4$ and carbon particles will ensure structural stability during cycling, and the expansion of $NiCo_2O_4$ particles can be absorbed by elastic carbon.

Conclusions

In summary, $NiCo_2O_4$/C nanocomposite was successfully prepared by a convenient hydrothermal method followed by a simple calcination process. Under 40 mA/g current density, 958.4 mAh/g reversible capacity can be obtained and the capacity retention was 78.3% after 50 cycles. It was noted that the initial coulombic efficiency can reach as high as 79.2%. The excellent electrochemical performance of the $NiCo_2O_4$/C nanocomposite could be mainly attributed to the high distribution of $NiCo_2O_4$ particles within the carbon matrix and a good interface affinity between the $NiCo_2O_4$ and carbon particles, which resulted from the in situ preparation of $NiCo_2O_4$ and carbon. Carbon in the nanocomposites provided a good conductive matrix, which not only kept the integrity, but also decreased the polarization of the anode, thus enhancing the capacity retention of the electrode.

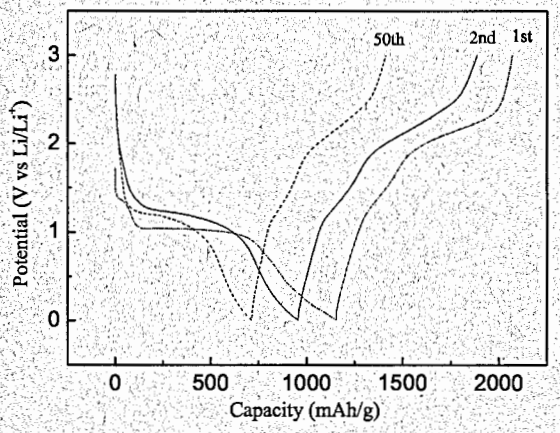

Figure 5. Charge–discharge curves of the $NiCo_2O_4$/C nanocomposite electrode at 40 mA/g.

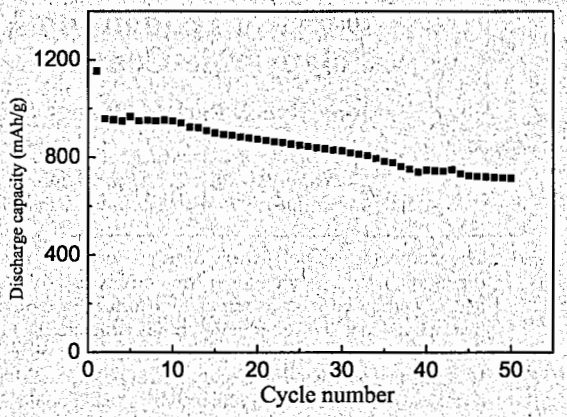

Figure 6. Discharge capacity vs cycle number curve of the $NiCo_2O_4$/C nanocomposite electrode at 40 mA/g.

Acknowledgments

This work was financially supported by the Australian Research Council through a Linkage Project (LP0775456).

Shanghai Jiao Tong University assisted in meeting the publication costs of this article.

References

1. Y. Idota, T. Kubota, A. Matsufuji, Y. Mackawa, and T. Miyasaka, *Science*, **276**, 1395 (1997).
2. J.-M. Tarascon and M. Armand, *Nature (London)*, **414**, 359 (2001).
3. P. Poizot, S. Laruele, S. Grugeon, L. Dupont, and J.-M. Tarascon, *Nature (London)*, **407**, 496 (2000).
4. X. H. Huang, J. P. Tu, C. Q. Zhang, and J. Y. Xiang, *Electrochem. Commun.*, **9**, 1180 (2007).
5. R. Alcántara, M. Jaraba, P. Lavela, and J. L. Tirado, *Chem. Mater.*, **14**, 2847 (2002).
6. R. Alcántara, M. Jaraba, P. Lavela, J. L. Tirado, J. C. Jumas, and J. Olivier-Fourcade, *Electrochem. Commun.*, **5**, 16 (2003).
7. P. Lavela and J. L. Tirado, *J. Power Sources*, In press online.
8. X. H. Yang, X. Wang, and Z. D. Zhang, *J. Cryst. Growth*, **277**, 467 (2005).
9. Y. Ch. Chu, Zh. W. Fu, and Q. Z. Qin, *Electrochim. Acta*, **49**, 4915 (2004).
10. H. K. Xin, W. Q. Fu, Z. X. Guang, and W. X. Lei, *J. Electrochem. Soc.*, **153**, A1568 (2006).
11. C. C. Hu and C. Y. Cheng, *Electrochem. Solid-State Lett.*, **5**, A43 (2002).
12. K. W. Nam, W. S. Yoon, and K. B. Kim, *Electrochim. Acta*, **47**, 3201 (2002).
13. A. Iida and R. Nishikawa, *Jpn. J. Appl. Phys., Part 1*, **33**, 3952 (1994).
14. Zh. Fan, J. H. Chen, K. Z. Cui, F. Sun, Y. Xu, and Y. F. Kuang, *Electrochim. Acta*, **52**, 2959 (2007).
15. R. R. Owings, G. J. Exarhos, C. F. Windisch, P. H. Holloway, and J. G. Wen, *Thin Solid Films*, **483**, 175 (2005).
16. R. R. Owings, P. H. Holloway, G. J. Exarhos, and C. F. Windisch, *Surf. Interface Anal.*, **37**, 424 (2005).
17. B. Chi, J. B. Li, Y. Sh. Han, and Y. J. Chen, *Int. J. Hydrogen Energy*, **29**, 605 (2004).
18. K. Byrappa and T. Adschiri, *Prog. Cryst. Growth Charact. Mater.*, **53**, 117 (2007).